RASĀYAN *J. Chem.*
Vol. 17 | No. 2 |436-442| April - June | 2024
ISSN: 0974-1496 | e-ISSN: 0976-0083 | CODEN: RJCABP
http://www.rasayanjournal.com
http://www.rasayanjournal.co.in

PREPARATION AND FLAME RETARDANT APPLICATION OF CLAY POLYURETHANE NANOCOMPOSITES

P. Kamalarajan✉ and S. Ramesh
Department of Chemistry, R.M.D. Engineering College,
Kavaraipettai-601206, (Tamil Nadu) India
✉Corresponding Author: kamal.snh@rmd.ac.in

ABSTRACT

In recent years, clay-based organic thermosetting polyurethane polymer nanocomposites have more attracted attention in academia and industries because they exhibit different properties from conventional materials. In this study, we investigated novel thermoplastic Polyurethane (TPU) by adding nanoparticles of clay as a fire-retardant property. By employing an in-situ polymerization technique with a 2:1 ratio of tolylene 2,4-diisocyanate (TPI) and polyethylene glycol (PEG2000), the NCO terminated TPU prepolymer was created. Cloisite 25A (C25A), an organo-modified montmorillonite clay, was utilized to provide sufficient compatibility with the PEG/TPI matrix. The synthesized nanocomposite was examined using thermogravimetric analysis (TGA), SEM analysis, and X-ray diffraction (XRD). FTIR analysis provides information on functional groups. Compared to pure polyurethane, the nanocomposites showed superior thermal stabilities, as determined by thermogravimetric analysis (TGA). The results from X-ray diffraction and Scanning Electron Microscopy confirm the successful formation of an exfoliated polymer clay nanocomposite under all conditions, evidenced by the absence of the distinct peak ($2\theta = 4.79^{o}$) corresponding to the d-spacing of the organoclay. The relationship between clay loading and TPU matrix type and the mechanical characteristics of nanocomposites was examined. As the amount of clay in the Young's TPU/Cl25A nanocomposites grew, so did their tensile strength and modulus. The fire-retardant experiment was studied by a cone colorimeter. There have been notable advancements in the fire-retardant qualities, including smoke, CO output, and heat release rate. Comparing polyurethane integrated with 5-weight percent organoclay to ordinary polyurethane polymer, a noteworthy 53% reduction was observed.

Keywords: Organoclay, Nanocomposites, Polyurethane, Flame-Retardant, Cloisite 25A.
RASĀYAN *J. Chem.*, Vol. 17, No. 2, 2024

INTRODUCTION

In the past few decades, a novel class of materials called organic polymer-layered silicate nanocomposite has emerged. According to their original polymer, such composites' characteristics were substantially enhanced. Because of strong interactions between the components, they offer better properties than traditional materials. They can be produced cheaply and easily.[1,2] Numerous consumer items, including barrier layer materials, drink packaging, protective coatings, bottle applications, and adhesive molding compounds, employ polymer/clay nanocomposite.[3] Clay mineral-based reinforcement materials are frequently utilized to enhance the thermal, tensile, barrier, flame resistance, dyeability, and several other characteristics of polymers.[4] Clay minerals' density, tiny cost, high accessibility, large surface area, and aspect ratio, which enhance the polymer's properties, are the major reasons why they are used as strengthening materials. A 2:1 phyllosilicate, montmorillonite (Mt) is one of the minerals. Cloisite 25A (Cl25A) is an organoclay made from hydrogenated tallow alkyl bis (hydroxyethyl) methyl quaternary ammonium-reinforced polymeric matrices. Compared to other organo-modified clays like cloisite 20A and cloisite 10A, Cl25A is compatible with polyurethane (Pu).[5] Polyurethane is a block copolymer with sections that alternate between strength and flexibility. The semicrystalline tough segments originate from the interaction of diisocyanate and diol, while the amorphous soft segments are derived from long-chain polyols.[6] The kinds of raw resources used, their makeup, and the processing circumstances may all affect how Pu behaves. Due to their adaptability, Pu is frequently utilized as coatings, adhesives, sealants, foams, and textiles. Due to their poor gas barrier qualities, PU clay materials have received research. The primary cause of Pu's poor gas barrier qualities is its micro-phase separation, which causes the two segments' polarity and thermodynamic incompatibility to differ.[7]

http://doi.org/10.31788/RJC.2024.1728754

By altering the raw ingredients and their compositions, several studies and scientific investigations have focused on enhancing the gas barrier property of PU.[8] Additionally, a lot of studies have used graphene-based or nano-sized clay to improve the barrier-to-gas permeation capabilities of PU. Chen et al. made this observation when comparing a nanocomposite made of PU and benzidine using a solution method.[9] The characteristics of the resulting polymer clay nanocomposites are greatly improved by the processing method. Numerous academic publications claim that solution mixing produces superior outcomes to melt mixing. One of the predominant challenges persisting in melt mixing remains the dispersion of clay grains within the polymer matrix. the most significant issue with melt mixing is still the dispersion of clay grains in the polymer matrix.[10] According to Finnigan *et al.* stress, strain properties, and elongation decreased as a result of Pu breakdown during the blending process when 7% and 3% of the weight of cloister 30B were added to TPU.[11] Solution blending was utilized to achieve a homogeneous nano-sized clay distribution in the Polyurethane phase. According to Bapan Adak *et al.,* there is a relationship between the He gas barrier characteristics of Pu nanocomposites and two distinct organoclays.[12] In this research, we combined Clay and polyurethane nanocomposites utilized to provide fire resistance. The impact of nanoclay on the morphological and mechanical qualities of PU/C25A nanocomposites was assessed. To our knowledge, no studies have been conducted on how organo-modified clay affects the behavior of the material used in PU/Cl25A nanocomposites.

EXPERIMENTAL

Material and Methods

Every reagent has an analytical purpose. Fluka, India is the source of both the 2,5-Dihydroxybenzenesulfonic acid potassium salt acid, and the polyethylene glycol (PEG2000). Sigma Aldrich, an Indian company, sells 4-Methyl-1,3-phenylene diisocyanate (TDI) and isophorone-diisocyanate (IPDI). Fluka provides access to butyltin-dilaurate (DBTDL). Formyldimethylamine was acquired from Elim Chem Pvt Ltd in Hyderabad, India, in HPLC grade. Southern Clay, USA provided the Cloisite 25A (sodium montmorillonite modified with 2-ethylhexyl quarternary ammonium cation and dimethyl hydrogenated tallow). To reduce the water content of the clay, it was first dried for six hours at 80 ºC in a hot air oven. We utilized dimethylformamide (DMF) from Merck, India, with no more treatment.

TPU Clay Nanocomposites Synthesis

The instructions in the preceding literature create the TPU clay nanocomposite. Within a tripartite reaction kettle, 6g of polyethylene glycol was added and dissolved in dimethylformamide. A determined amount of tolylene 2,4-diisocyanate (TDI) and cloisite 25A (1 wt.% regarding the monomer) was introduced gradually to a reaction vessel after polyethylene glycol swelled in DMF. To extend the chain, the hydroquinone sulphonic acid of potassium salt had to be dissolved in DMF and then applied dropwise at 50 degrees Celsius. The method of N-Butylbutan-1-amine and the isocyanate disappearance group's IR absorption at 2271 cm^{-1} were used to calculate the theoretical isocyanate concentration of 4-5%, and the heating was maintained until this level was obtained. The reaction mixture undergoes heating to 80 degrees Celsius in a nitrogen gas atmosphere for four hours. To create a Thermoplastic PU/Cl25A nanocomposite thin film, the emulsion is applied to a Teflon mould. The test is conducted once again using clay weight percentages of three, five, and seven, the resultant nanocomposite material undergoes drying and is subjected to a variety of analytical procedures to describe it. Table-1 lists the codes and composition of the nanocomposite.

Table-1: Formulation of TPU Clay Nanocomposites

Specimen code	Composition				
	NCO: OH Mol ratio	*TDI*	*PEG*	*Closite Wt.%*	*Regid Segment (mol%)*
Neat TPU	1.01	70	30	0	24
TPU/Cl25A-1	1.11	70	30	1	25
TPU/Cl25A-3	1.33	70	30	3	26
TPU/Cl25A-5	1.52	70	30	5	27
TPU/Cl25A-7	1.73	70	30	7	28

Characterization Techniques

Nicolet 400D impact FT-IR spectrometer is used to examine the clay nanocomposite's FT-IR spectra. The Rigaku Miniflex 600 diffractometer (operating at 30 kV, 10 mA) is used to measure the X-ray

crystallography method (XRD) in the nanocomposites and the clay was scanned at a rate of 2°C per minute at room temperature. The value range of which the spectra are recorded is 0 to 15 degrees. Use Bragg's equation to determine the nanocomposites' basal spacing. X-ray diffraction is used to evaluate the composite specimens using films that are 2 mm thick and are produced by compression molding at 180 °C. Using a Perkin Elmer Thermal Gravimetric Analysis (TGA) instrument, the investigation of polymer clay nanocomposites' thermal stability occurs at a heating value rate of 20 °C. per minute in a nitrogen gas environment. At room temperature, the specimen was heated to 800 °C. Images of the fractured surfaces of tensile specimens were captured by scanning electron microscopy with a JEOL JEM-5800 at a 20 kV acceleration voltage. A UTM Universal Testing Machine is used to evaluate mechanical testing (Instron-3369, UK). When the crosshead is moving at 50 mm per minute, 100 N of force is being exerted. The ASTM D: 638 test methods specify the use of dumbbell-shaped specimens having thicknesses ranging from 1.1 to 2.9 mm, 15 mm at each end, and 10 mm at the neck. Cone calorimeters were used to measure the flammability characteristics in line with ISO 5660. (Stanton Redcroft, England).

RESULTS AND DISCUSSION

FT-IR analysis was employed to examine the structural properties of nanocomposites comprising TPU and C25A. The functional groups are revealed using an FT-IR spectrometer. FT-IR spectrum was procured for the materials under investigation in the temperature range of 4000-500 cm^{-1} at normal temperature. Figure-1 represents the infrared spectra of nanocomposites involving TPU and TPU1. The NH bending of primary amine stretching vibration of the urethane group, attributed to the interaction between NCO and OH groups, manifests as a distinctive peak at 3300 cm^{-1}. Specific absorption bands in the TPU spectra include 1642 cm^{-1} (O-H deformation), 3402 cm^{-1} (H_2-bonded water), and 3754 cm^{-1} (O-H stretching out vibration of Aluminium -OH groups). The unique bond at 1721 cm^{-1} is associated with the carbonyl stretching vibrational frequency of acetic acid. Additionally, various bands are discernible at different wavelengths, such as 676 cm^{-1} (Methylene out-of-plane bending), 1158 cm^{-1} (C-O stretching vibration), 1440 cm^{-1} (CH bending vibration), 1378 cm^{-1} (Methylene plane scissoring vibration), and 2953 cm^{-1} (CH_2 symmetric stretching vibration). Distinctive absorption bands for TPU/C25A nanocomposites encompass the methylene vibration of the benzene ring at 660 cm^{-1}, Methylene stretching from 2975 to 2888 cm^{-1}, silica asymmetric stretching at 1088 cm^{-1}, and the Carbonyl stretching of the acetate group at 1259, 1088, and 1018 cm^{-1}. Notably, the CH stretching of the nanocomposite remains unchanged, indicating the unaffected state of the clay particle when bonded to urethane -NH groups. The FT-IR spectra convincingly demonstrate a robust interaction and effective complexation between the clay and polymer.

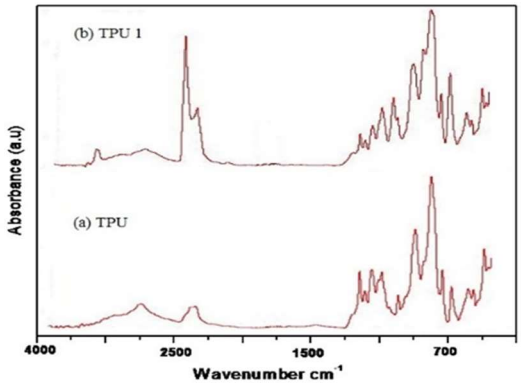

Fig.-1: The FTIR Spectra for Thermoplastic Polyurethane and Clay Cl25A Nanocomposite

XRD analysis was employed to investigate the nano clay dispersion type in the polymer matrix and the alteration in TPU's crystal shape due to the presence of nano clay. Figure-2 illustrates wide-angle XRD patterns of the TPUA/Cl25A nanocomposite at various weight percentages and pure clay. Polymer chains are introduced between the clay layers to create polymer/clay nanocomposites with increased gallery space. The basal spacing (d001) is ascertained using Bragg's law with XRD measurements. A change in the peak in the clay's d001 peak in the XRD spectrum signifies an intercalated structure, whereas the lack of this peak hints at an exfoliated structure in nanocomposites. The silicate-interlayer spacing value of 18.3 Å,

correlated with a characteristic 001 peak at 2θ = 4.79º in the foundational spacing is adjusted for organomodified MMT clay (cloisite 25A). For TPU/Cl25A nanocomposites, the distinct peak of clay cloisite 25A is missing till to an angle of 4º, indicating that cloisite 25A achieves almost complete exfoliation within the TPU matrix. These findings suggest a uniform exfoliation of clay content, randomly distributed throughout the TPU matrix.

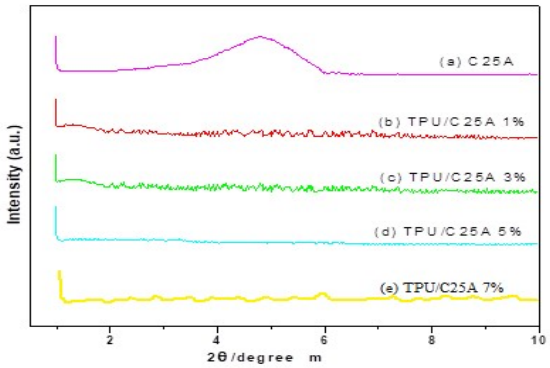

Fig.-2: The XRD Spectrum of (a) Cl25A Clay and Different Molar Ratio of Cl25A Nanocomposites b) Neat TPU/Cl25A 1% (c)TPU/Cl25A 3% (d) TPU/Cl25A 5% (e) TPU/Cl25A 7%

Figure-3 presents the TGA thermograms of TPU and TPU/Cl25A at 20°C in a nitrogen atmosphere with varying weight percentages of clay nanocomposites, and Table-2 provides the corresponding values. Organoclay influences the thermal stability of nanocomposites in two ways: catalyzing polymer degradation and enhancing stability through oxygen barrier properties. In this study, it is observed that the barrier effect prevails, owing to the limited amount of clay incorporated into the polymer phase. Neat Thermoplastic PU/Cl25A exhibits thermal degradation in two stages, with the first involving the removal of acetate groups at temperatures up to 310–410°C, followed by the deterioration of the core restraint as the second matrix. Nanocomposites did not experience weight loss below 207°C, and decomposition commenced around 300°C. TPU is found to be entirely anhydrous with decent thermal stability. Furthermore, TPU/Cl25A materials show a difficult heat breakdown temperature (308°C) compared to TPU adduct (reported at 207°C). At 800°C, TPU/Cl25A nanocomposite materials leave a scum of approximately 22%, while the TPU adduct leaves about 19%. These results suggest that 88% of the original clay incorporation was quantitatively absorbed as an exfoliated structure into the TPU adduct, potentially influencing the high-temperature breakdown behavior of TPU/Cl25A nanocomposites. Scanning electron microscopy (SEM) is employed in the initial phase to assess the dispersion of enhanced clay in TPU nanocomposites. In Fig.-4, scanning electron images depict TPU with varying clay weight contents. In contrast to morphology images by SEM of neat Thermoplastic PU and TPU/Cl25A nanocomposite materials, the clay particles are distinctly visible and evenly distributed throughout the TPU matrix structure, accompanied by small agglomerates. These clay particles exhibit sizes ranging from 0.5 to 10 micrometers. The enhanced contacts among the organic polymer and clay contribute to a more uniform distribution of Closite within the Thermoplastic PU phase. The images show a roughly grainy surface coating, indicating an even distribution of clay fillers throughout the TPU matrix. Any unevenness on the surface may be attributed to the solute cross-linking action. Moreover, SEM images clearly indicate that clay fillers at 1%, 3%, and 5% weight are freely dispersed throughout the TPU matrix, displaying an exfoliated structure. The results confirm that the synthesized nanocomposites have a size of 100 nm.

Table-2: Characteristics of Thermal decomposition of Thermoplastic PU/Cl25A Nanocomposites

Temp	Nanocomposites with different wt.% clay content				
	TPU	1%	3%	5%	7%
T_1 ºC	207.42	308.24	331.46	356.76	341.68
T_2ºC	402.34	492.43	505.07	532.36	512.42
Residue wt.%	19.24	21.47	24.87	27.27	23.62

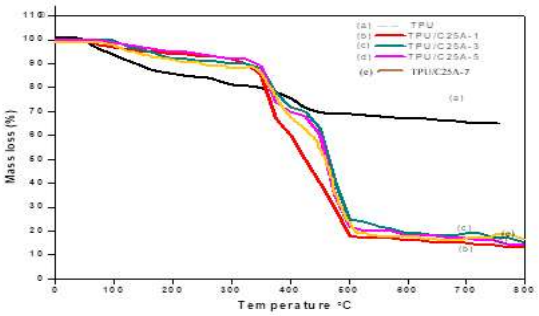

Fig.-3: The TG Curves of (a) Thermoplastic PU (b) TPU/Cl25A 1% (c) TPU/Cl25A 3% (d) TPU/Cl25A 5% (e) TPU/Cl25A 7% Nanocomposites Materials

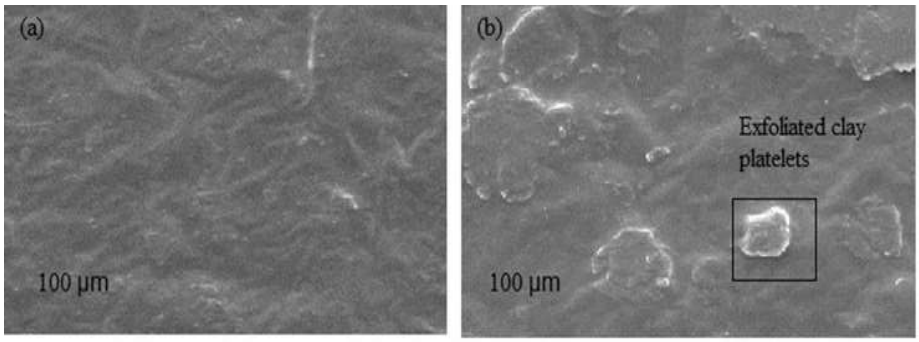

Fig.-4: SEM images of TPU/C25A Nanocomposite

Figure-5 provides a summary of the mechanical parameters for TPU/Cl25A nanocomposites, with Table-3 presenting the results of tensile strength stress and strain (TS) and percentage Stretch at break tests (EB). The Fig.-5 illustrates an increase in both tensile strength and percentage Stretch at the break as the clay content rises to 5 weight percent. Combining TPU and Cloisite 25A has generally produced layers of modified organophilic silicates with significant interfacial contact and polymer chain diffusion. The nanocomposite is therefore expected to be able to bear a higher external load than pure TPU. The addition of 5% clay to neat Thermoplastic PU results in a change in ductile strength to 13.2 MPa, marking an 80% increase compared to pure TPU. This enhancement can be attributed to the assimilation of uniformly discrete clay into the TPU matrix, thereby strengthening and reinforcing the material. In composites with an aggregated clay content of 7 weight percent or more, the TS and EB begin to deteriorate, which causes poor contact between the TPU and clay layers. Table-3 presents the Young's modulus of the TPU with various percentages of clay weight. The results indicate that the presence of closite25A may restrict the molecular movement chain of the polymer, leading to decreased flexibility and increased stiffness in the material. The research findings highlight that while nano clay contributes synergistically to increased tensile strength, it concurrently reduces the flexibility of the polymer significantly.

Table-3: Mechanical Characteristics of Thermoplastic PU/Clay Nanocomposites

Samples	σ (MPa)	E (MPa)	ε (%)
Neat TPU	8.1	12.2	658
TPU/Cl25A-1	9.4	17.3	736
TPU/Cl25A-3	11.6	21.2	810
TPU/Cl25A-5	13.2	24.3	948
TPU/Cl25A-7	12.8	20.2	902

The flammability assessment of TPU/C25A nanocomposites was conducted using the cone calorimeter. Figure-6 depicts the kinetic heat release rate (HRR) peaks for both neat Thermoplastic PU and TPU of varying Cl25A contents. In the case of pure TPU, a distinct HRR peak is observed with a curve HRR (PHRR) amount of 1859 kW/m2. Additionally, pure TPU exhibits a 72-second ignition period and a relatively brief 200-second burning duration. While the PHRR values decrease with an increase in clay concentration, the HRR curve of the flame-retardant materials appears sleek, with PHRR values lower than

657 kW/m2. Furthermore, the non-flammable carbon dioxide and the water vapor generated during the breakdown of TPU nanomaterials contribute to the dilution of combustible gases and the deceleration of gas phase burning. According to cone calorimetric tests, the TPU/C25A nanocomposite's peak heat release rate (PHRR) is 53% lower than that of pure TPU.

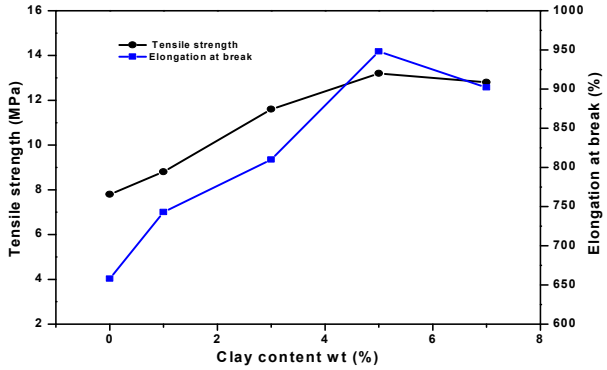

Fig.-5: Mechanical Properties Versus Clay in Thermoplastic PU/Cl25A Nanocomposites

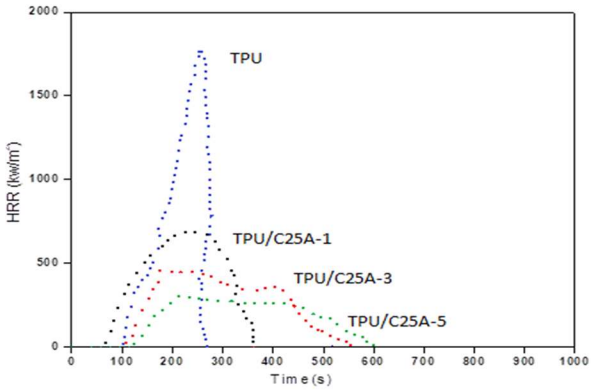

Fig.-6: HRR Curves of TPU, TPU/C25A1, TPU/C25A3, and TPU/C25A5 Nanocomposites

CONCLUSION

Solution polymerization was used to prepare TPU/Cl25A nanocomposites successfully. The interaction of clay and polyurethane has demonstrated how oxygen and nitrogen permeability can be increased in composite materials. Infrared data have confirmed the robust contact and effective complexation between the organic polymer and organoclay. Through XRD and SEM analyses, it is evident that the synthesized nanocomposite materials are exfoliated and uniformly distributed throughout the organopolymer main chain. TGA testing demonstrates enhanced heat stability in the nanocomposite compared to pure TPU polymer. Additionally, mechanical research indicates that as the clay content increases, Tensile strength Young's modulus, and elongation at break also increase. Cone calorimetric measurements reveal that the TPU/Cl25A nanocomposite exhibits a peak value of heat release rate (HRR) that is 53% lower than the virgin material.

ACKNOWLEDGMENTS

The Central Leather Research Institute (CLRI) provided all of the characteristic analysis, and the authors are grateful to the Research and Development Centre at Bharathiar University for their generous support.

CONFLICT OF INTERESTS

The authors hereby affirm that they have no conflicts of interest to disclose.

AUTHOR CONTRIBUTIONS

All the authors contributed significantly to this manuscript, participated in reviewing/editing, and approved the final draft for publication. The research profile of the authors can be verified from their ORCID IDs, given below:

P. Kamalarajan https://orcid.org/0000-0001-5202-8302
S. Ramesh https://orcid.org/0000-0003-0238-2869

REFERENCES

1. A. Dorigato, A. Pegoretti and A. Penati, *Journal of Reinforced Plastics and Composites*, **30**, 4(2011), https://doi.org/10.1177/073168441039659
2. T. Allami, A. Alamiery, M. H. Nassir and A. H. Kadhum, *Polymers*, **13**, 5(2021), https://doi.org/10.3390/polym13152467
3. S. Chaitoglou, L. Spachis, G. Zisis, I. Raptis, N. Papanikolaou, A. Vavouliotis, R. Penedo, N. Fernandes and A. Dimoulas, *Progress in Organic Coatings,* **150**, 1(2021), https://doi.org/10.1016/j.porgcoat.2020.105984
4. T. Saliney, T. Shaji, A. Jiji, C. G. Soney and T. Sabu, *Journal of Polymer Research*, **25**, 8(2018), https://doi.org/10.1007/s10965-018-1562-y
5. R. Goyat, Y. Saharan, J. Singh, A. Umar and S. Akbar, *Molecules,* **27**, 19(2022), https://doi.org/10.3390/molecules27196433
6. B. Adak, M. Joshi, and B. S. Butola, *Journal of Applied Polymer Science*, **135**, 27(2018), https://doi.org/10.1002/app.46422
7. G.V.R. Reddy, M. Joshi, B. Adak and B. L. Deopura, *Coloration Technology*, **134**, 2(2018), https://doi.org/10.1111/cote.12332
8. H. Kim, Y. Mitura and C.W Mascosko, *Chemical Engineering and Materials Science,* **22,** 11(2010), https://doi.org/10.1021/cm100477v
9. S. Peretz Damari, L. Cullari, R. Nadiv, Y. Nir, D. Laredo, J. Grunlan and O. Regev, *Composites Part B: Engineering*, **134**, 1(2018), https://doi.org/10.1016/j.compositesb.2017.09.056
10. J. Reza, E. Behnam and T. Hamed, *Arabian Journal for Science and Engineering*, **42**, 4401(2017), https://doi.org/10.1007/s13369-017-2498-y
11. A. Amari, F. M. Alzahrani, K. M. Katubi, N.S. Alsaiari, M.A. Tahoon and F.B. Rebah, *Materials*, **14**, 6(2021), https://doi.org/10.3390/ma14061365
12. M. Gholami and G.M. Sadeghi, *Journal of Particle Science & Technology*, **1**, 1(2015), https://doi.org/10.22104/JPST.2015.64
13. S. Rathi and J.B. Dahiya, *Advanced Materials Letters*, **3**, 5(2012), https://doi.org/10.5185/amlett.2012.5354
14. M. Rafiee, F. Nitzsche, J. Laliberte, S. Hind, F. Robitaille and M.R. Labrosse, *Composites Part B: Engineering,* **164,** 1(2019), https://doi.org/10.1016/j.compositesb.2018.11.051
15. Y. Ahmadi, M. Yadav and S. Ahmad, *Composites Part B: Engineering,* **164**, 1(2019), https://doi.org/10.1016/j.compositesb.2019.01.078

[RJC- 8754/2023]